

# Aerosol concentration over Ranchi urban area and South Karanpura Coalfield region, Jharkhand, India-A comparative geospatial appraisal

Akshay Kumar\* and Akhouri Pramod Krishna

Department of Remote Sensing, Birla Institute of Technology, Mesra, Ranchi- 835215, Jharkhand, India

\*Corresponding Author: akshay61296@gmail.com

---

## ABSTRACT

Atmospheric aerosols are known to influence the air quality in urban, rural and mining regions of the world. The present study investigates the concentration of aerosol optical thickness (AOT) measured at 40 locations in Ranchi urban area (RUA) within urban boundary layer and 42 locations in South Karanpura Coalfield region (SKCR) to quantify the atmospheric conditions over the region. Aerosol concentration has been measured by using a five channel (340-1020 nm) handheld microprocessor-based MICROTUPS-II Sunphotometer during the peak winter season, in the month of January 2014. It is observed that AOT concentration is higher (1.92-3.33 at 340 nm) in the vicinity of thermal power plant, sponge iron factory, mining area, coal-based small industries and construction sites, whereas lower (<1.50) in the forest and low population density areas and within agricultural lands. In comparison with the urban area of Ranchi city, AOT concentration showed variation with high values (0.68-0.34 at 340 nm) at main centers of railway and road traffic junctions, whereas lower concentration (<0.34) in the residential area. The AOT values are higher for smaller wavelengths (340 nm) and lower for higher wavelengths (1020 nm) indicating the dominance of fine particles in the atmosphere compared to larger size particles. We have also derived Ångström parameters ( $\alpha$ ,  $\beta$ ) for the wavelength pair 340-870 nm. Results show that the values of ' $\alpha_{340}$ ' have a range of 0.47 to 2.59 and 0.60 to 1.04 in mining region and RUA, respectively. The values of ' $\beta$ ' have a range of 0.03 to 1.92 and 0.07 to 0.20, respectively. This study suggests that the aerosol concentration is higher over mining region as compared to urban areas due to the expansion of industries and coal mining activities over the years.

**Key words:** Aerosol optical thickness, MICROTUPS-II Sunphotometer, Ångström exponent, GIS, Coal mining, Urban area.

---

## INTRODUCTION

Aerosols are also known as particulate matter (PM), a primary pollutant that affects air quality in urban, rural and mining areas of the world (Gupta et al., 2006). It is a complex mixture of extremely tiny solid and liquid particles that vary in sizes (extending from  $10^{-2}\mu\text{m}$  to  $10^2\mu\text{m}$ ) and composition and remains suspended in the air (Ranjan et al., 2007; Kumar and Krishna, 2017). Aerosol optical thickness (AOT) is the vertical aerosol loading, present in the atmosphere and directly correlated with solar radiation by way of scattering and absorption processes (Ranjan et al., 2007). Primary aerosols are formed from natural sources such as volcanic emissions, dust storms, forest and grassland fires, living vegetation and sea spray. Whereas, secondary aerosols are originating from anthropogenic sources such as the burning of fossil fuels and alteration of natural surface covers (Kaskaoutis et al., 2007). Atmospheric aerosols affect air quality, human health and radiation budget of the earth (IPCC, 2007). Loading of higher aerosol concentration also causes a substantial decrease in sunlight reaching the land surface, which affects vegetation because of its dependence on sunlight

for their growth (Prasad et al., 2006). These environments may influence human health, especially respiratory system through inhalation of fine particulate matter. Also, aerosols could reduce the physical visibility due to scattering and absorption of radiation (Dockery and Pope, 1994). Thus, mesoscale assessment of AOT in any area provides the status of air pollution in the region.

The Ranchi city has a significant influence on the socio-economic factors of the region due to its highest accessibility and possession of infrastructure. It is performing all the central functions of a society (Kumar and Pandey, 2013a). The rapid growth (39.0%) of built-up area in and around Ranchi Township, since its inception as the state capital in the year 2000, happened due to absence of a proper urban town/ city planning. This is evident in terms of increase in vehicular pollution and mushrooming of high-rise buildings, largely along the main roads and river beds (Kumar and Pandey, 2013a). Compared to Ranchi Township, South Karanpura is one of the most productive coalfields of the Jharkhand state employing both sub-surface and opencast mining techniques. Such a large-scale mining practice has led to significantly more environmental pollution, particularly deterioration in air

quality by dust and gaseous pollutants (Armstrong et al., 1980; Kumar et al., 2016; Kumar and Pandey, 2013b). Air pollution problem is not only within the mining area but also in the surrounding locations. The relationship between coal mining activities and aerosol concentration were also investigated by several researchers (Chadwick et al., 1987; Munroe et al., 2008). They found that biomass burning and mining-related activities (blasting, transportation, dumping) are responsible for air pollution in the region.

Wavelength dependence of scattering and absorption effects of aerosols is illustrated by Ångström wavelength exponent ( $\alpha$ ) and Ångström turbidity ( $\beta$ ) formula (Ångström 1964). In recent past, several studies have been conducted on various aspects of Ångström exponents (O'Neill et al., 2001; Kalapureddy and Devara, 2008). They described Ångström exponents as a tool to estimate particle size distribution, extrapolating AOT throughout the broad spectral region to distinguish the different aerosol types (Kumar and Krishna, 2017). The relationship between the wavelength ( $\alpha$ ) and turbidity ( $\beta$ ) follows a power law called Ångström power law. It seems to be a good representation of aerosol that has a wide variety of origins and compositions (McCartney, 1976). Kumar and Pandey, (2013a) have retrieved and analyzed the spatial distribution of various environmental indicators such as ambient air quality, aerosol concentration, ambient noise level and urban green space over Ranchi City, Jharkhand. The AOT concentration is higher at transport and road junctions ( $>0.30\%$  at 340 nm), and low levels ( $<0.22\%$  at 340 nm) at residential areas. To have a comparison with other cities we have studied the variability of AOT concentration and Ångström parameters over Varanasi (Tiwari and Singh, 2013). Tiwari and Singh (2013) have observed that AOT concentration has increased during the pre-monsoon and winter season.

The remote sensing (RS) and geographic information system (GIS) are established techniques for monitoring and interpretation of the spatial distribution of atmospheric aerosols and their characteristics over the area. The aim of the present study is to use geospatial technology for investigating the column aerosol optical properties such as AOT and Ångström exponent using measurements of MICROTOPS-II Sunphotometer over Ranchi city or Ranchi urban area (RUA) and South Karanpura Coalfield region (SKCR). So as to effectively collect good quality data and analyze the same properly we have carried out detailed literature survey to gather relevant information covering aerosols impact in different environments. Useful information has been gathered from an interesting study in Rajkot. Ranjan et al., (2007) investigated aerosol concentration over Rajkot city during July 2004 to July 2005 using MICROTOPS-II Sunphotometer. They observed that AOT exhibits seasonal variation with high values during summer (0.41) and low values during winter (0.11).

The present research work also analyses the prime causes behind increasing AOT concentration over the urban and mining area. Further, environmental changes in both the areas need to evaluate and suggest control measures for their adverse effects.

## Study Area

The area taken for the present study is Ranchi city and a coal mining impacted region (South Karanpura Coalfield). Ranchi is the capital city of Jharkhand state, situated ( $23^{\circ}13-23^{\circ}26$  N latitude and  $85^{\circ}13-85^{\circ}26$  E longitude) on the Chotanagpur plateau in the eastern part of India at an elevation of 650 m above mean sea level (Figure 1). The study area is delineated based on 2 km outer buffer of the Ranchi Municipal Corporation (RMC) boundary that occupies 317.62 km<sup>2</sup> area. The SKCR (40 km away from Ranchi, on the northern side) is situated in parts of Ramgarh and Hazaribagh districts of Jharkhand state, India (Figure 1). The total area covered by SKCR is about 380 km<sup>2</sup> as delineated from the Survey of India (SOI) topographical map (Sheet No. 73 E/6) on a scale of 1:50,000, lies between  $23^{\circ}35'$  to  $23^{\circ}44'$  N latitude and  $85^{\circ}15'$  E to  $85^{\circ}27'$  E longitude and is about 348m above mean sea level. It is a hilly area, a part of the Chotanagpur plateau, covered with lush green forest. Fertile land is partly cultivated and the agriculture is mostly rain fed. The climate of the study area is tropical and has three seasons; summer, winter and monsoon. The area receives mean annual rainfall of 1400 mm and the temperature reaches up to 45°C during summer and falls to 2°C during winter.

## Instrumentation and Data

In the present study, hand-held multiband MICROTOPS-II Sunphotometer (Solar Light Company, USA) has been used for measurement of AOT concentration during the month of January 2014. It provides measurements of AOT, direct solar irradiance in each band and columnar water vapor (also called precipitable water). A global positioning system (GPS) (Trimble GeoExplorer 3000 GeoXT series) has been used to obtain real-time data on sub-foot ( $<30$  cm) horizontal and 2-3 m post-processed vertical accuracy (Pandey and Kumar, 2013). The Sunphotometer is equipped with five accurately aligned optical collimators at 340, 500, 870, 936 and 1020 nm wavelengths, with collimator 2.5° field of view, a narrow-band interference filter and a photodiode suitable for each wavelength range. A Sun target and pointing assembly are permanently attached to the optical block and laser-aligned to ensure accurate alignment with the optical channels. The calibration procedure and instrument uncertainties are discussed in detail by Morys et al., (2001).

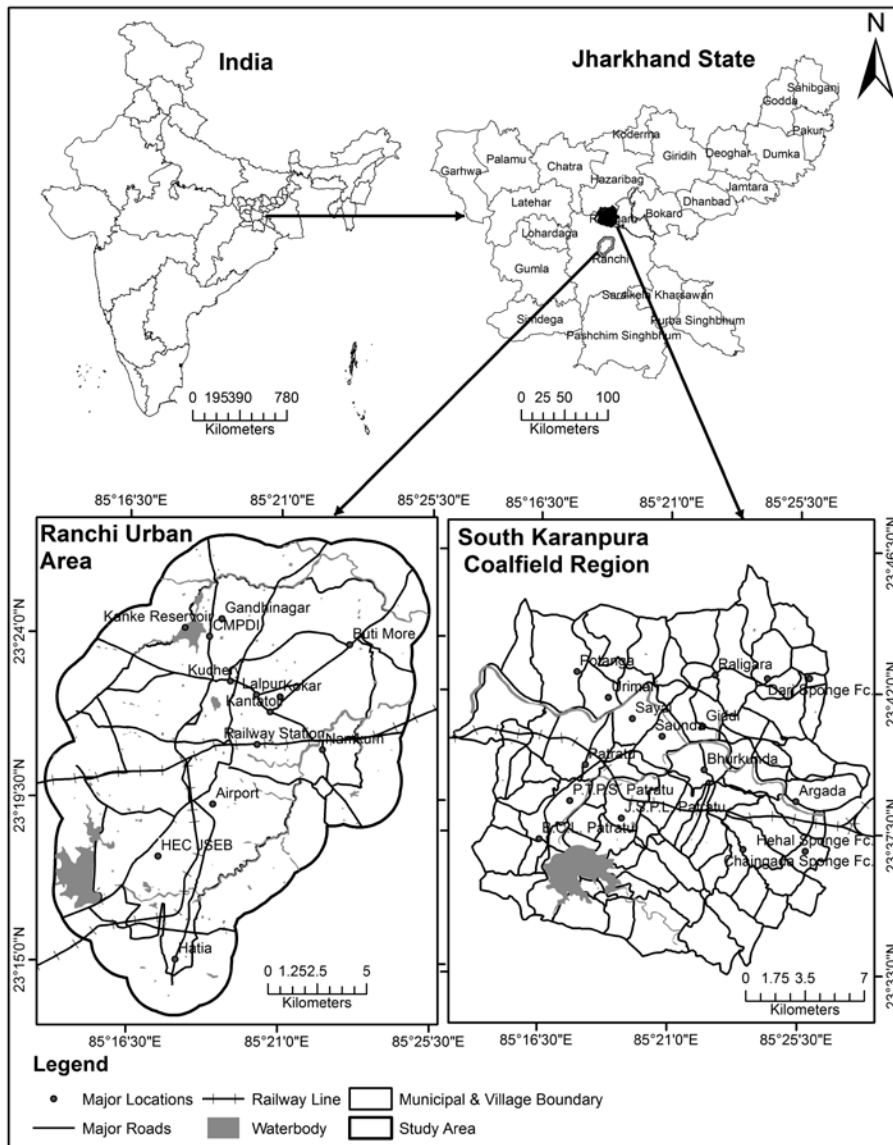


Figure 1. Location map of the study area.

## METHODOLOGY

The AOT is the most simple and important parameter to characterize and determine aerosols in the atmosphere (Gómez-Amo et al., 2008). It can be obtained as the immediate result of solar radiation extinction measurements by using the Bouguer-Lambert-Beer law, expressing total attenuation of the direct solar beam through the atmosphere (Gómez-Amo et al., 2008):

$$V_{\lambda} = V_{0\lambda} D^{-2} \exp [-\tau_{\lambda} (M)] \quad (1)$$

Where,  $V_{\lambda}$  = signal measured by the instrument at wavelength  $\lambda$ ,  $V_{0\lambda}$  = extraterrestrial signal,  $D$  = Earth-Sun distance in Astronomical Units at time of observation,  $\tau_{\lambda}$  = total optical thickness ( $\tau_{\lambda} = \tau_{a\lambda} + \tau_{R\lambda} + \tau_{O3\lambda}$ ),  $\tau_{a\lambda}$  = aerosol

optical thickness,  $\tau_{R\lambda}$  = Rayleigh (air) optical thickness,  $\tau_{O3\lambda}$  = Ozone optical thickness,  $M$  = the optical air mass. The spatial distribution of AOT was recorded at 40 locations in RUA and 42 locations in SKCR in the month of January 2014. At each site, five samples have been collected, and their average values are used. All the observations are done during clear sky conditions, which imply the cloud-free days or proper sunshine (during 10:00 to 16:00 h). The recorded values of AOT at observation sites are interpolated in GIS environment by importing it from GPS-derived geographic locations of sample points. The spatial pattern of AOT over study area is analyzed using the inverse distance weightage (IDW) algorithm of GIS.

The Ångström exponent ( $\alpha$ ,  $\beta$ ) is the simplest representation of the spectral variation of aerosol optical

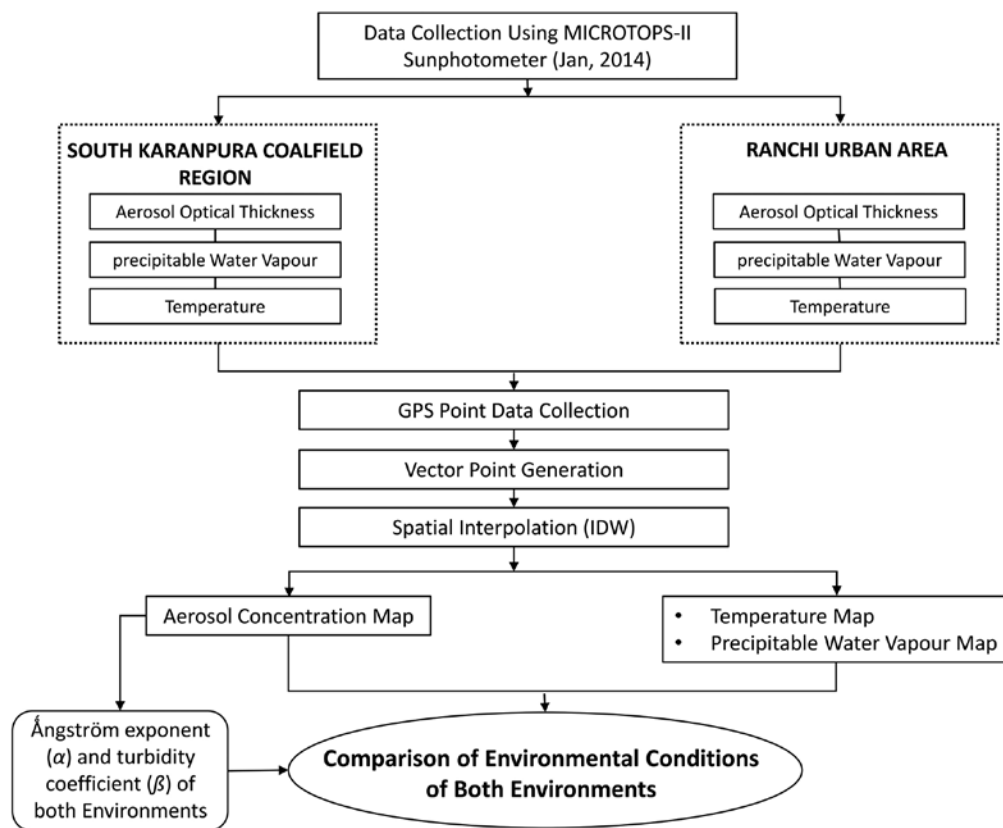


Figure 2. Methodology flow chart.

thickness ( $\tau$ ) using Ångström empirical formula. It is determined from the spectral dependence of the measured optical thickness data. The coefficient of Ångström exponent ( $\alpha, \beta$ ) is computed using the Ångström empirical formula (Ångström, 1964). It is given by the Equation 2:

$$(\tau) = \beta \lambda^{-\alpha} \tag{2}$$

Where,  $\lambda$  = wavelength in micrometer,  $\tau$  = AOT,  $\alpha$  = Ångström exponent,  $\beta$  = turbidity coefficient, which is equal to columnar AOT at  $\lambda = 1 \mu m$ . The wavelength of  $\alpha$  and  $\beta$  are independent, exhibiting spectral variation depending upon the aerosol physical and chemical characteristics (Eck et al., 1999). The exponent ' $\alpha$ ' represents the aerosol size distribution, whereas ' $\beta$ ' is related to the aerosol loading (Badarinath et al., 2008). The Angstrom wavelength exponent ( $\alpha$ ) can be calculated using the AOTs ( $\tau$ ) at two different wavelengths by using equations 3 and 4:

$$\tau_1 = \beta * \lambda_1^{-\alpha} \tag{3}$$

$$\tau_2 = \beta * \lambda_2^{-\alpha} \tag{4}$$

From which,

$$\tau_1/\tau_2 = (\lambda_1/\lambda_2)^\alpha = (\lambda_2/\lambda_1)^{-\alpha} \tag{5}$$

$$Ln (\tau_1/\tau_2) = \alpha Ln (\lambda_2 - \lambda_1) \tag{6}$$

For solving  $\alpha$ ,

$$\alpha = Ln (\tau_1/\tau_2) / Ln (\lambda_2 / \lambda_1) \tag{7}$$

For the natural environments, ' $\alpha$ ' ranges from 0.5 to 2.5 with an average of  $1.3 \pm 0.5$ . Larger values of ' $\alpha$ ', when the ' $\tau$ ' value for the larger wavelength is much smaller than the ' $\tau$ ' value for the shorter wavelength, imply a relatively high ratio of small particles to large particles ( $r > 0.5 \mu$ ). As ' $\tau$ ' values for the greater wavelength approach the ' $\tau$ ' values of the shorter wavelength, the larger size particles dominate the distribution causing smaller ' $\alpha$ ' values. It is not possible for the ' $\tau$ ' value of the larger wavelength to equal or become greater than the ' $\tau$ ' value of a short wavelength.  $\beta$  has been calculated from wavelength (340 nm):

$$\beta = \tau_1 * \lambda_1^\alpha = \tau_2 * \lambda_2^\alpha \tag{4}$$

Where  $\lambda$  is in microns ( $340 \text{ nm} = 0.340 \mu$ ). ' $\beta$ ' values of less than 0.1 are associated with a relatively bright atmosphere, and values greater than 0.2 are associated with a moderately hazy atmosphere. The detailed methodology adopted in the present study is shown in Figure 2.

**Table 1.** Statistics of AOT and Angstrom parameters over South Karanpura coalfield region (SKCR) and Ranchi urban area (RUA) during January 2014.

Wavelengths/ Parameters	Min		Max		Mean		Std. deviation	
	SKCR	RUA	SKCR	RUA	SKCR	RUA	SKCR	RUA
AOT 340	0.511	0.209	3.333	0.839	1.113	0.366	0.783	0.185
AOT 500	0.213	0.151	2.999	0.797	0.787	0.291	0.766	0.193
AOT 870	0.077	0.088	2.555	0.772	0.503	0.219	0.654	0.214
AOT 936	0.104	0.088	2.565	0.747	0.505	0.208	0.615	0.197
AOT 1020	0.102	0.086	2.574	0.693	0.526	0.200	0.605	0.188
Angstrom Exponent ( $\alpha_{340-870}$ )	0.472	0.401	2.593	2.204	1.490	0.859	0.640	0.302
Turbidity Coefficient ( $\beta_{340}$ )	0.031	0.063	1.923	0.531	0.388	0.164	0.506	0.138

## RESULTS AND DISCUSSION

### Spatial variability of aerosol concentration

The concentration of AOT was measured at 40 locations in RUA and 42 locations in SKCR during the winter period of January 2014. The spatial pattern of AOT distribution analyzed using geographical information system (GIS), revealed variations in the AOT concentration at all five wavelengths ranging from 340 to 1020 nm (Figure 3). The spatial distribution map of all wavelengths for both environments indicates that the value of AOT concentration for shorter wavelength (340 nm) is higher as compared to longer wavelength (1020 nm). It shows that the regions were indicating a dominance of finer size particles over larger size in the atmosphere. The AOT concentration over SKCR shows a significant variation, compared to RUA (Figure 3). The concentration of AOT over RUA lies between 0.086-0.839 and between 0.077-3.333 over SKCR. The AOT loading of all wavelengths (340-1020 nm) was found to be enhanced over SKCR as compared to RUA. The mean value of AOT 340 nm is 1.113. The standard deviation is 0.783 over SKCR. Over RUA, mean value is 0.366 and the standard deviation 0.185. Average AOT concentration of all wavelengths (340-1020 nm) over RUA is lower than the mean level over SKCR. It indicates that the environmental conditions are more severe over SKCR. The statistics of aerosol concentration for both the periods and at all wavelengths (340-1020 nm) are shown in Table 1. The AOT (340-1020 nm) concentration over RUA has been found to be higher at major commercial centers, railway and road traffic junctions (Railway station, Khelgoan, Main road, Kanke), whereas it is lower in planned residential areas (Gandhinagar and HEC Sector III) (Figure 3). In SKCR, the AOT (340-1020 nm) has been found to be greater at industrial zones (P.T.P.S., J.S.P.L., Bhurkunda, Chaingada, Dari and Hehal), followed by mining areas such as Potanga, Railgada, Sayal, Saunda, Sirka, Giddi-C and Bhurkunda colliery. Such trends may be due to the high frequency of transportation activities, loading/

unloading of coal and smoke emissions from coal-based industries causing high dispersions of dust particles into the atmosphere. Whereas it is lower in the residential areas. A high value of AOT at lower wavelengths shows that at both the observation sites, the small size particles are dominant. The gradual decrease of AOT with increasing wavelengths suggests that the aerosol size distribution of this site is according to the Junge's inverse power law distribution (Ranjan et al., 2007):

$$\frac{dn}{dr} = Cr^v \quad (9)$$

Where, C represents a constant depending on the total number of particles. The average AOT concentration has been analyzed, and it indicates that small size particles are dominated by coarser size, over both the areas. Mean AOT concentration of all wavelengths (340-1020 nm) is also higher in SKCR as compared to RUA. Thus, the urban environment of Ranchi city is comparatively better than the adjacent SKCR with respect to aerosol concentration in the atmosphere. The concentration of finer size particles in RUA is attributed primarily to vehicular pollution, whereas in coalfield region, they mostly originate from thermal power plants and allied industries.

### Relationship between AOT concentration and meteorological parameters

Aerosol monitoring is better achieved by the combined use of ground-based measurements of aerosol properties in conjunction with surface meteorological data. Aerosol concentration is influenced by airflow, atmospheric humidity, temperature and other weather conditions. The associated meteorological parameters such as relative humidity (RH, %), accumulated rainfall (RF, mm) and wind speed (WS, m/s) have been downloaded from <http://global-weather.tamu.edu/> over study area for ten years (2005-2014) on a daily basis. Relative humidity (RH) of both areas varied from 45-55%, whereas annual rainfall data indicates that there is negligible rainfall during January. Average value of

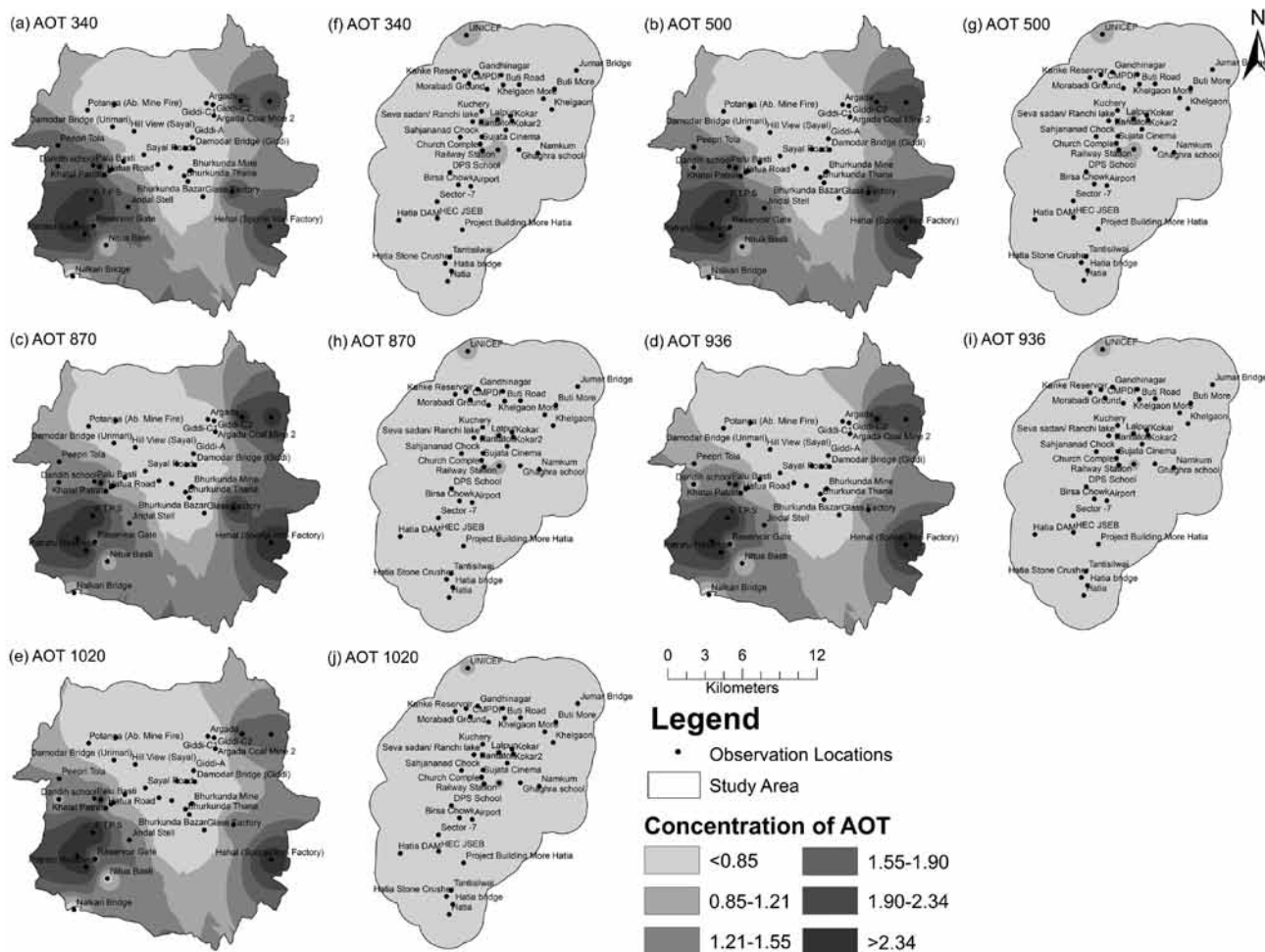


**Figure 3.** Variation of AOT at different wavelengths over South Karanpura Coalfield region (a-e) and Ranchi urban area (f-i).

wind speed during the study period is 2.42 m/s, showing less dust transport at the measurement site. Meteorological conditions are stable and impose minor influence on the carriage of aerosols from neighboring areas and can be considered mainly from local land surface processes.

Precipitable water vapour (PWV) and temperature data for each location have been simultaneously recorded during AOT measurements. Spatial distribution map of PWV and temperature are shown in Figure 4. The data indicates that the PWV concentration over SKCR varied from 0.30 to 1.80 cm with a mean value of 0.83 cm. Over RUA, it ranges from 0.2 to 0.45 cm, with an average value of 0.32 cm. The temperature varied between 15.1°C to 26.0°C in SKCR and between 17.9°C to 23.5°C in RUA. The mean value of temperature in SKCR and RUA is 21.9°C and 20.9°C, respectively. Figure 4a demonstrates that the maximum concentration of PWV over SKCR is higher on the western side along with some portion of northern and eastern parts due to the presence of coal-based industries, whereas over RUA the PWV concentration shows less variation compared to SKCR (Figure 4b). The

spatial variation of average temperature in SKCR exhibited west to east gradient, whereas temperature in RUA indicated north to south gradient (Figures 4c & d). The relationship between AOT340 concentration and PWV has been examined through regression analysis of both the environments. The  $R^2$  value for SKCR and RUA was 0.84 and 0.71 respectively, ascertain the relationship between AOT and PWV concentrations in the area. Some of the earlier studies (Ranjan et al., 2007; Kumar and Pandey, 2013a; Kumar et al., 2016) also indicate that water vapour significantly contributes to AOT concentration, whereas it does not have a positive relationship with temperature.

### Ångström Parameters

Ångström exponent ( $\alpha$ ) and turbidity coefficient ( $\beta$ ) are other two important parameters for studying the atmospheric aerosol properties along with AOT. Latah and Badrinath (2004) pointed out that significant value of ' $\alpha$ ' indicates a relatively high ratio of small particles to large particles. If the size of air molecules and aerosol particles are equal, then ' $\alpha$ ' should be near 4. For larger particles,

Aerosol concentration over Ranchi urban area and South Karanpura Coalfield region, Jharkhand, India-A comparative geospatial appraisal

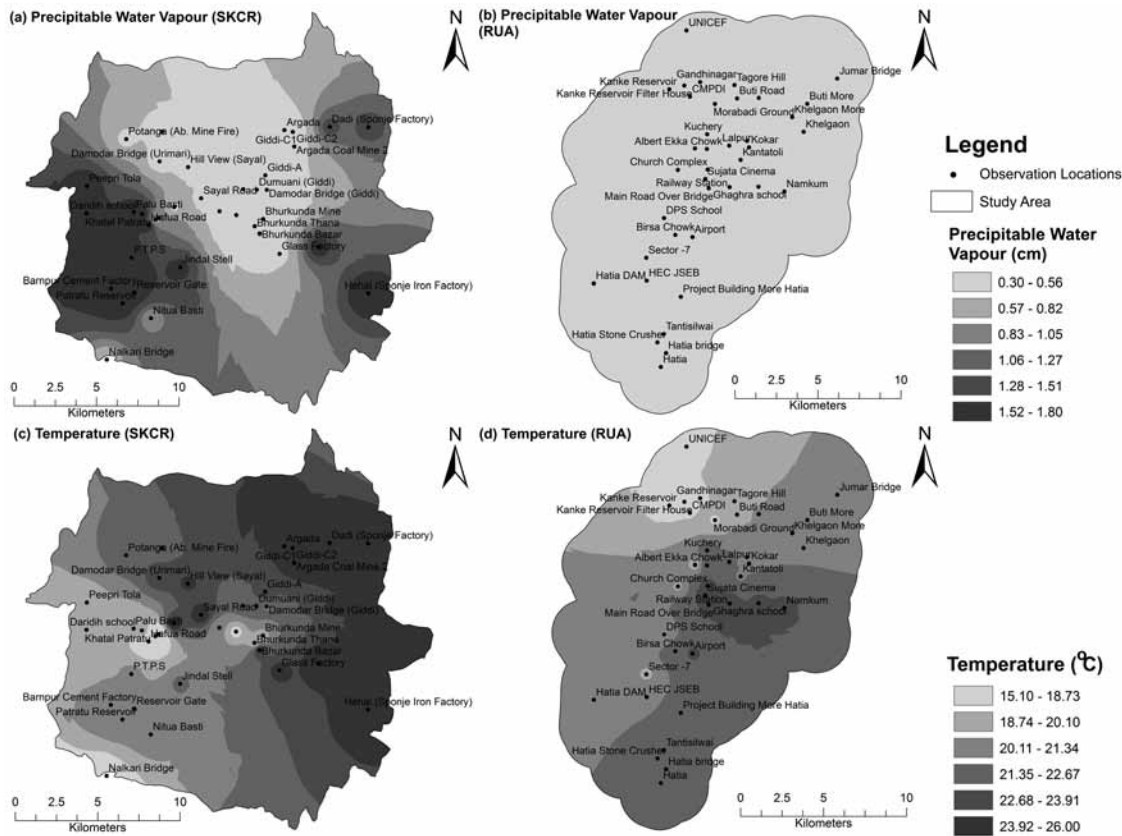


**Figure 4.** Variations of precipitable water vapour (a, b) and temperature (c, d) as recorded by Sunphotometer over South Karanpura Coalfield region and Ranchi urban area.

it should be approximately 0. Thus, the greater value of ‘ $\alpha$ ’ indicates the dominance of small size particles that produce scattering in the region. The turbidity coefficient ( $\beta$ ) gives an estimate of aerosol loading over the site (Ranjan et al., 2007).

The amount of aerosol present in the atmosphere is indicated by parameter ‘ $\tau$ ’ and the aerosol size distribution is indicated by ‘ $\alpha$ ’ (Tiwari and Singh, 2013). Here, ‘ $\alpha$ ’ and ‘ $\beta$ ’ are calculated for wavelength pair 340 and 870 nm and plotted for both the regions for the determination of aerosol size distribution and total columnar aerosol loading over SKCR and RUA (Figures 5a & b). The higher value of ‘ $\alpha$ ’ implies the dominance of smaller size aerosol particles and vice versa. The value of  $\alpha_{340-870}$  over SKCR lies between 0.472 to 2.593, with mean and standard deviation of 1.490 and 0.640, respectively. The range  $\alpha_{340-870}$  is 0.401 to 2.204, with mean value equal to 0.859, and standard deviation of 0.302 over RUA. It indicates that different sizes of aerosols are present in the atmosphere over the region. From Figure 5b, the relatively higher values of ‘ $\alpha$ ’ (1.490) on an average indicate that the existence of smaller size aerosol particles may be due to industrial pollution from Power plant, Sponge iron factory and Steel plant. Aerosols are also generated by biomass burning. Aerosols

are also due to dust coming from coal mining activities. It is observed that average value of ‘ $\alpha$ ’ is relatively higher, on the other hand over RUA, ‘ $\alpha$ ’ mean value (0.859) is small i.e.  $\alpha < 1.0$  ( $r = 0.5 \mu\text{m}$ ), indicating that larger aerosol particle size is dominant.

The variation of the turbidity coefficient ( $\beta$ ) values lie between 0.031 to 1.923 and 0.063 to 0.531 over SKCR and RUA, respectively. The mean value of  $\beta_{340}$  is 0.388 and 0.164 during SKCR and RUA. The standard deviation of SKCR and RUA is 0.506 and 0.138, respectively. This signifies the nature of variation of AOT over two different environments. It is observed that the variation of ‘ $\alpha$ ’ is almost opposite in nature to that of ‘ $\beta$ ’ i.e. higher values of ‘ $\alpha$ ’ are associated with the lower values of ‘ $\beta$ ’. Thus, the present study concludes that ‘ $\alpha$ ’ and ‘ $\beta$ ’ are negatively correlated to each other, which is in agreement with the earlier observations (Satheesh et al., 2006; Reddy et al., 2011). Statistical analysis of Ångström parameters are shown in Table 1. The aerosols over SKCR is dominated by biomass-burning aerosols, which are characterized by a thick atmosphere consisting of high value ( $>1.5$ ) of  $\alpha$ . The spectral features depend on a type of combustible process. Age of aerosols and humidity causes injection of a vast number of fine particles into the atmosphere (Toledano et

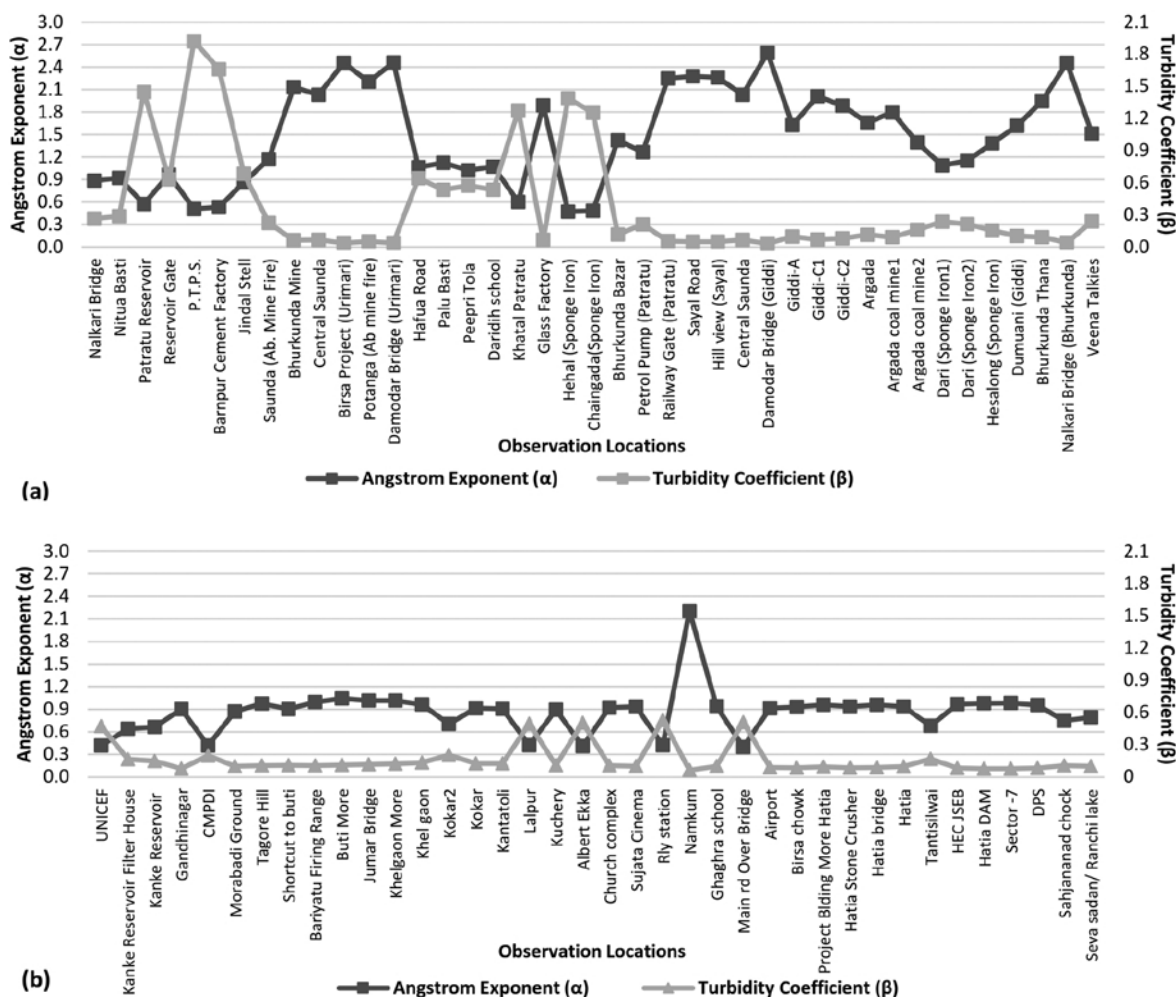


**Figure 5.** Variation of Ångström exponent ( $\alpha$ ) and Turbidity coefficient ( $\beta$ ) over (a) South Karanpura Coalfield region and (b) Ranchi urban area.

al., 2007). Thus, the higher AOT conditions with strong wavelength dependence create high  $\alpha$  values ( $>1.5$ ) over the area (O'Neill et al., 2001).

### CONCLUSION

Aerosol concentration and their size characteristics over Ranchi city and South Karanpura Coalfield region have been studied. The maximum level ( $>3.0$ ) is observed over SKCR near the industries (P.T.P.S., Hehal, Chaingada, Bhurkunda, etc.) followed by coal mining area (Potanga, Railgada, Sirka and Giddi-C). In RUA, it is found to be maximum ( $>0.7$ ) near massive transport junctions. Lower AOT concentration ( $<1.0$ ) is noted near forest areas and planned residential area, followed by settlement and water body in both the environments. Ångström parameters ( $\alpha$ ,  $\beta$ ) values extend between 0.472-2.593 and 0.031-1.923 over SKCR, whereas they lie between 0.401-2.204 and 0.063-0.531 over RUA. It indicates the presence of different

particle sizes of aerosols (mostly fine-mode particles) in both the environments. Comparative evaluations revealed that the AOT concentration over SKCR (0.51-3.33) is higher than RUA (0.20-0.83) during the winter season. Aerosols influence and impact in different seasons may be useful in better visualizing the spatio-temporal variations in the two environments investigated in the present study. This will be taken up as an extension of the present study.

The outcome of this study provides a quantitative assessment of the environmental conditions of both the regions and can help in the formulation of environmental development policy.

### ACKNOWLEDGEMENT

Authors express sincere thanks to Centre of Excellence in Climatology, Birla Institute of Technology, Mesra for providing MICROTUPS-II Sunphotometer used in this study. Authors are also grateful to Mr. Atul Kumar

Tiwari and Mr. Sams Raza for their assistance during data acquisition over the study area. The first author gratefully acknowledges receipt of the Institute fellowship of the Birla Institute of Technology, Mesra, Ranchi to carry out the present research under a PhD program. The authors profusely thank Dr. P. Sanjeeva Rao, editorial board member of JIGU for his critical review of the manuscript, which significantly helped to improve the quality of the manuscript. Thanks are due to Chief Editor for his kind support and detailed final editing.

### Compliance with Ethical Standards

The authors declare that they have no conflict of interest and adhere to copyright norms.

### REFERENCES

- Ångström, A., 1964. The Parameters of Atmospheric Turbidity. *Tellus*, v.16, pp: 64-75.
- Armstrong, J.A., Russel, P.A., and Darmel, D.C., 1980. Particle from Surface Mining, Part I-Vertical Measurements, Report No. EPA-600=9-80-041 (Research Triangle Park, NC: USEPA, Industrial Environmental Research Laboratory).
- Badarinath, K.V.S., Kharol, S.K., Prasad, V.K., Sharma, A.R., Reddi, E.U.B., Kambezidis, H.D., and Kaskaoutis, D.G., 2008. Influence of Natural and Anthropogenic Activities on UV Index Variations—A Study over Tropical Urban Region Using Ground Based Observations and Satellite Data, *Journal of Atmospheric Chemistry*, v.59, pp: 219-236.
- Chadwick, M.J., Highton, N.H., and Lindman, N., 1987. Environmental Impacts of Coal Mining and Utilisation. A Complete Revision of Environmental Implications of Expanded Coal Utilization. Pergamon Press, England.
- Dockery, D.W., and Pope, C.A., 1994. Acute respiratory effects of particulate air pollution, *Annual review of public health*, v.15, no.1, pp: 107-132.
- Eck, T.F., Holben, B.N., Reid, J.S., Dubovik, O., Smirnov, A., O'Neill, N.T., Slutsker, I., and Kinne, S., 1999. Wavelength Dependence of the Optical Depth of Bio Mass Burning: Urban, and Desert Dust Aerosols. *Journal of Geophysical Research*, v.104(D-24), pp: 31333-31349.
- Gupta, P., Christopher, S.A., Wang, J., Gehrig, R., Lee, Y.C., and Kumar, N., 2006. Satellite remote sensing of particulate matter and air quality over global cities. *Atmospheric Environment*, v.40, no.30, pp: 5880-5892.
- Gómez-Amo, J.L., Estellés, V., Pedrós, R., Utrillas, M.P., Sobrino, J.A., and Martínez-Lozano, J.A., 2008. Column aerosol characterization in a semi-arid region around Marrakech during the WATERMED 2003 campaign. *International Journal of Remote Sensing*, v.29, no.17-18, pp: 5013-5027.
- Intergovernmental Panel on Climate Change (IPCC): Climate Change, 2007. The Physical Science Basis: Contribution of Working Group I to the Fourth Assessment Report of the Intergovernmental Panel on Climate Change, Cambridge University Press, Cambridge, United Kingdom and New York, USA.
- Kaskaoutis, D.G., Kambezidis, H.D., Hatzianastassiou, N., Kosmopoulos, P.G., and Badarinath K.V.S., 2007. Aerosol Climatology: On the Discrimination of the Aerosol Types over four AERONET Sites. *Atmospheric Chemistry and Physics Discussions*, v.7, no.3, pp: 6357-6411.
- Kalapureddy, M.C.R., and Devara, P.C.S., 2008. Characterization of aerosols over oceanic regions around India during pre-monsoon 2006. *Atmospheric Environment*, v.42, no.28, pp: 6816-6827.
- Kumar, A., and Pandey, A.C., 2013a. Spatio-temporal Assessment of Urban Environmental Conditions in Ranchi Township, India using Remote Sensing and Geographical Information System Techniques. *International Journal of Urban Sciences*, DOI.org/10.1080/12265934.2013.766501., v.17, no.1, pp: 117-141,
- Kumar, A., and Pandey, A.C., 2013b. Evaluating Impact of Coal Mining Activity on Land use/land cover using Temporal Satellite Images in South Karanpura Coalfields and Environs, Jharkhand State, India. *International Journal of Advanced Remote Sensing and GIS 2013*, Available online: <http://technical.cloudjournals.com/index.php/IJARSG/-article/view/Tech-110/pdf>, v.2, pp: 183-197.
- Kumar, A., Pandey, A.C., and Kumar, M., 2016. Evaluating Variability of Aerosol Concentration in Coal Mining Areas: A Case Study from Patratu Coal Mining Region, Jharkhand. *Int. Conference Geological Society of India*, DOI: 10.17491/cgsi-2016/95904., pp: 119-129.
- Kumar, A., and Krishna, A.P., 2017. Winter seasons assessment of atmospheric aerosol over Coalfield region of India using geoinformatics. *Urban Climate*, v.20, pp: 94-119.
- Latah, K.M., and Badrinath, K.V.S., 2004. Association of Aerosol Optical Depth with near Surface Aerosol Properties in Urban Environment. *Indian Journal of Radio & Space Physics*, v.33, no.4, pp: 256-259.
- McCartney, E.J., 1976. Optics of the atmosphere: scattering by molecules and particles. John Wiley and Sons. New York, pp: 421.
- Morys, M., Mims, F.M. III, Hagerup, S., Anderson, S.E., Baker, A., Kia, J., and Walkup, T., 2001. Design, Calibration, and Performance of MICROTOS-II Handheld Ozone Monitor and Sun Photometer. *Journal of Geophysical Research*, v.106, pp: 14573-14582.
- Munroe, D.K., Wolfenbarger, S.R., Calder, C.A., Shi, T., Xiao, N., Lam, C.Q., and Li, D., 2008. The relationships between biomass burning, land-cover/use change, and the distribution of carbonaceous aerosols in mainland Southeast Asia: a review and synthesis. *Journal of Land Use Science*, v.3, no.2-3, pp: 161-183.
- O'Neill, N.T., Eck, T.F., Holben, B.N., Smirnov, A., Dubovik, O., and Royer, A., 2001. Bimodal Size Distribution Influences on the Variation of Angstrom Derivatives in Spectral and

- Optical Depth Space, *Journal of Geophysical Research: Atmospheres*, v.106 (D9), pp: 9787-9806.
- Prasad, A.K., Singh, R.P., and Singh, A., 2006. Seasonal climatology of aerosol optical depth over the Indian subcontinent: trend and departures in recent years. *International Journal of Remote Sensing*, pp: 2323-2329, DOI: 10.1080/01431160500043665., v.27, no.12.
- Pandey, A.C., and Kumar, A., 2013. Analysing topographical changes in open cast coal-mining region of Patratu, Jharkhand using CARTOSAT-I Stereopair satellite images. *Geocarto International*, DOI: 10.1080/10106049.2013.838309.
- Ranjan, R.R., Joshi, H.P., and Iyer, K.N., 2007. Spectral Variation of Total Column Aerosol Optical Depth over Rajkot: A Tropical Semi-arid Indian Station. *Aerosol Air Quality and Research*, v.7, no.1, pp: 33-45.
- Reddy, B.S.K., Kumar, K.R., Balakrishnaiah, G., Gopal, K.R., Reddy, R.R., Reddy, L.S.S., Narasimhulu, K., Rao, S.V.B., Kumar T.K., Balanarayana, C., and Moorthy, K.K., 2011. Aerosol Climatology over an Urban Site, Tirupati (India) Derived from Columnar and Surface Measurements: First Time Results Obtained from a 30-Day Campaign. *Journal of Atmospheric and Solar-Terrestrial Physics*, v.73, no.13, pp: 1727-1738.
- Satheesh, S.K., Deepshikha, S., and Srinivasan, J., 2006. Impact of Dust Aerosols on Earth atmosphere Clear-sky Albedo and Its Short Wave Radiative Forcing over African and Arabian Regions. *International Journal Remote Sensing*, v.27, pp: 1691-1706.
- Toledano, C., Cachorro, V.E., Berjon, A., De Frutos, A.M., Sorribas, M., De la Morena, B.A., and Goloub, P., 2007. Aerosol optical depth and Ångström exponent climatology at El Arenosillo AERONET site (Huelva, Spain). *Quarterly Journal of the Royal Meteorological Society*, v.133, no.624, pp: 795-807.
- Tiwari, S., and Singh, A.K., 2013. Variability of aerosol parameters derived from ground and satellite measurements over Varanasi located in the Indo-Gangetic Basin. *Aerosol Air Quality and Research*, <http://dx.doi.org/10.4209/aaqr.2012.06.0162>., v.13, pp: 627-638.

Received on: 6.9.16; Revised on: 7.10.16; Re-revised on: 8.5.17; Accepted on: 10.5.17